



Overstretching B-DNA: The Elastic Response of Individual Double-Stranded and Single-Stranded DNA Molecules

Author(s): Steven B. Smith, Yujia Cui and Carlos Bustamante

Source: *Science*, New Series, Vol. 271, No. 5250 (Feb. 9, 1996), pp. 795-799

Published by: [American Association for the Advancement of Science](#)

Stable URL: <http://www.jstor.org/stable/2889889>

Accessed: 14/04/2013 17:36

Your use of the JSTOR archive indicates your acceptance of the Terms & Conditions of Use, available at <http://www.jstor.org/page/info/about/policies/terms.jsp>

JSTOR is a not-for-profit service that helps scholars, researchers, and students discover, use, and build upon a wide range of content in a trusted digital archive. We use information technology and tools to increase productivity and facilitate new forms of scholarship. For more information about JSTOR, please contact support@jstor.org.



American Association for the Advancement of Science is collaborating with JSTOR to digitize, preserve and extend access to *Science*.

<http://www.jstor.org>

Overstretching B-DNA: The Elastic Response of Individual Double-Stranded and Single-Stranded DNA Molecules

Steven B. Smith, Yujia Cui, Carlos Bustamante*

Single molecules of double-stranded DNA (dsDNA) were stretched with force-measuring laser tweezers. Under a longitudinal stress of ~ 65 piconewtons (pN), dsDNA molecules in aqueous buffer undergo a highly cooperative transition into a stable form with 5.8 angstroms rise per base pair, that is, 70% longer than B-form dsDNA. When the stress was relaxed below 65 pN, the molecules rapidly and reversibly contracted to their normal contour lengths. This transition was affected by changes in the ionic strength of the medium and the water activity or by cross-linking of the two strands of dsDNA. Individual molecules of single-stranded DNA were also stretched giving a persistence length of 7.5 angstroms and a stretch modulus of 800 pN. The overstretched form may play a significant role in the energetics of DNA recombination.

The elastic properties of dsDNA (bending and twisting rigidity) affect how DNA wraps around histones, packs into phage heads, supercoils in vivo, bends upon interaction with proteins, and loops to connect enhancer and promoter regions. A simple way to explore DNA elasticity is to stretch a single macromolecule from both ends, measuring the force F as a function of its end-to-end distance (or extension Ex). In this experiment, the tension experienced by each subunit in the chain is equal to F applied at the polymer ends, while the local deformation of each subunit adds to yield a macroscopically observable change in Ex . The type of polymer and the range of forces used determine the nature and size of the chain subunits that are involved in the elasticity response of the molecule, and the type of elasticity being investigated.

The entropic elasticity of a stiff chain involves small deviations of the molecular axis due to thermal fluctuations. The direction of such a chain is correlated over a span called the persistence length, P , which defines the size of the subunits relevant in entropic elasticity. For dsDNA, P in 10 mM Na^+ is ~ 150 base pairs (bp). Relatively small forces are required to align elastic units of these dimensions ($\sim k_B T/P$, where k_B is the Boltzmann constant and T is temperature). The entropic elasticity of single dsDNA molecules has been explored in the range from 0.01 to 10 pN (1, 2). Intrinsic elasticity, however, entails much larger deviations of the molecule's local structure. The elastic units are much smaller (on the scale of the polymer units) and larger forces

must be used. Typically, the intrinsic elasticity becomes evident only when the normal contour length of the molecule is approached or exceeded.

Optical trapping of polystyrene beads (3, 4) is used here on λ -phage DNA to characterize the intrinsic elasticity of dsDNA. Under high forces, the DNA can be stretched beyond its B-form contour length, and a remarkable discontinuity in the elastic response of dsDNA occurs at 65 pN. At this force, the molecule abruptly, but reversibly, assumes an extended form about 1.7 times its B-form contour length. Moreover, single-stranded DNA (ssDNA) molecules were prepared and their elastic properties were characterized for forces of 0 to 80 pN.

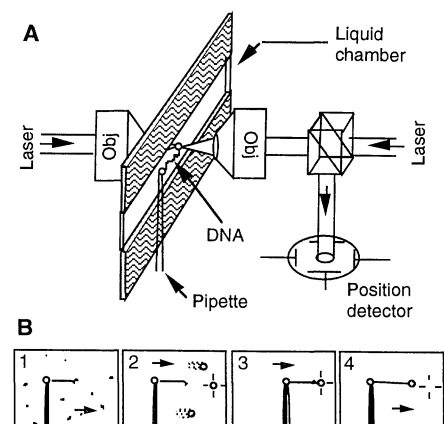
A dual-beam laser trap instrument was used to carry out these studies (Fig. 1A). Use of low numerical aperture (NA) lenses made it possible to hold beads deep inside a fluid cell, 100 μm away from the glass surfaces. Each end of a single λ -phage dsDNA mole-

cule (48.5 kbp) was attached to a separate microscopic latex bead (Fig. 1B). One bead was held by suction with a glass micropipette while the other bead was held in the optical trap, which also functioned as a force transducer. The DNA molecule was extended by moving the pipette relative to the laser trap. The extension of the DNA was determined from the distance between the beads with a video camera. The force acting on the DNA corresponding to each extension was inferred from the displacement of the laser beams on position-sensitive photodetectors. The force transducer was calibrated against the viscous drag on a bead by using Stokes' law but, alternatively, use of a dual beam trap makes it possible to calibrate it from first principles (conservation of light momentum) (5).

Typical F - Ex data are shown in Fig. 2 for a single molecule subjected to an extension-relaxation cycle in 150 mM NaCl buffer. The contour length of λ -DNA, assuming 3.38 $\text{\AA}/\text{bp}$, should be 16.4 μm . For lesser extensions, (10 to 15 μm), a small contractile force (< 5 pN) represents the entropic elasticity of dsDNA, in accordance with earlier studies (1). The force rises rapidly when the contour length is approached.

At forces < 50 pN, in which the DNA is still in its B form, the molecule displays an elastic stretch modulus, as evidenced by the difference between the theoretical behavior of an inextensible chain (2) (dashed line) and real DNA (dotted line) in Fig. 2. This elasticity, as averaged for 10 individual molecules in 150 mM Na^+ buffer, corresponds to a Young's modulus of $3.46^{+/-} 0.3 \times 10^8$ Pa, which would imply that P is 193 bp for dsDNA, assuming its radius is 10 \AA (6-8). Because the accepted value from electric birefringence and light-scattering methods (9) is ~ 150 bp at 0.1 M Na^+ , P would seem to be overestimated by the present method (10, 11).

Fig. 1. (A) Two diode lasers with 100-mW power and 800-nm wavelength (SDL-5311-G1) are oriented with orthogonally polarized beams. These beams converge to a common focus by means of two objective lenses (Nikon CF Plan Achromat 60x with correction, NA = 0.85), thus forming an optical trap. Only the rays exiting the trap are directed to position detectors (UDT SC-10D) by polarizing cube beamsplitters (only right cube and detector are shown). White-light illumination and video camera (not shown) are coupled through the objectives with dichroic beamsplitters, thus allowing measurement of the distance between bead centers. The molecular length is inferred from a set of such distances (27). **(B)** Bead-DNA assembly from solution. Arrows indicate buffer flow inside the fluid chamber. (1) DNA molecules are compact random coils in solution except when one attaches by an end to the bead on the pipette tip. (2) Extra beads are carried by buffer and one is caught by the laser trap. (3) The pipette is moved closer to the trap so DNA can span the gap. (4) The presence of the invisible DNA is evident because it pulls the bead upstream when the pipette is moved away from the trap (28).



S. B. Smith, Institute of Molecular Biology, University of Oregon, Eugene, OR 97403, USA.

Y. Cui, Institute of Molecular Biology and Physics Department, University of Oregon, Eugene, OR 97403, USA.

C. Bustamante, Institute of Molecular Biology, Chemistry Department, and Howard Hughes Medical Institute, University of Oregon, Eugene, OR 97403, USA.

*To whom correspondence should be addressed.

When $F \approx 65$ pN (Fig. 2), the molecule suddenly yields, lengthens, and eventually overstretches to ~ 1.7 times its B-form contour length, corresponding to an increase in the rise per phosphate from 3.4 to 5.8 Å. This transition occurs over a very narrow force range (~ 2 pN). The force rises rapidly again at extensions greater than 28 μm , indicating that the molecule is entirely converted to the overstretched form. The stretching cycle is reversed before 100 pN force is reached be-

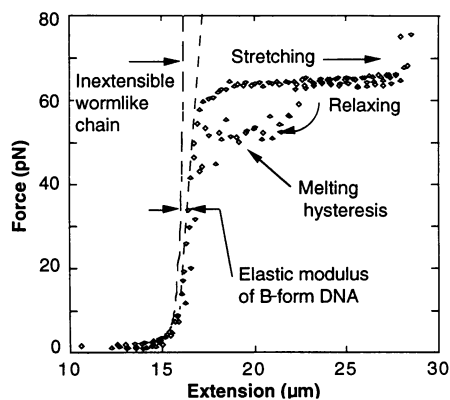


Fig. 2. Stretching of λ -phage DNA (NEB) in 150 mM NaCl, 10 mM tris, 1 mM EDTA, pH 8.0. The "inextensible wormlike chain" curve is from Bustamante *et al.* (2) for a P value of 53 nm and contour length of 16.4 μm .

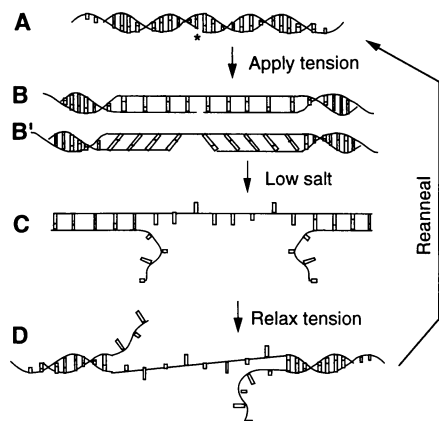


Fig. 3. (A) During the stretching part of a stretch-relaxation cycle, tension is applied to a nicked dsDNA molecule (* denotes nick). At some critical tension, dsDNA undergoes an overstretching transition. Two possible forms for overstretched dsDNA are shown. (B) The bases might unwind and unstack into a parallel ladder. Alternatively (B'), the bases could retain some partial stacking by slanting as in the "skewed ladder" model of Calladine and Drew (27). (C) If the overstretched dsDNA remains in low-salt buffer for more than a few seconds, then the nicked strand melts and frays back from both sides of the nick. (D) When the tension is released, the regions which have remained base-paired rapidly contract to B-DNA but the frayed regions take several minutes to reanneal, perhaps due to secondary structure in the frayed strands.

cause the biotin-streptavidin bond often breaks after a few seconds at this force.

Recently, several groups have stretched dsDNA far beyond B-form length using hydrodynamic or meniscus forces and leaving the stretched molecules adhered to a solid substrate. Using atomic force microscopy, Thundat *et al.* (12) observed λ -DNA on mica surfaces that had been stretched up to 1.8 times its B-form length during deposition. They proposed that the molecules unwound and the bases unstacked into a flat parallel ladder in which the bases pairs remained intact. The maximum length of such a ladder, obtained by optimizing backbone torsion angles while not opening tetrahedral angles (such as phosphate), is 2.1 times the B-form length. Other groups have observed dsDNA stretched up to 2 times (13) and 2.14 times (14) B-form length after deposition on a surface. The single-molecule manipulation approach used in the present study makes it possible to control the extension of the molecule and measure the equilibrium force needed for this extension. Under these conditions, overstretching is a highly cooperative, reversible transition (15).

During relaxation, the F - Ex curve often displays hysteresis (Fig. 2). This response is displayed repeatedly by any given molecule but varies considerably between different molecules. As diagrammed in Fig. 3, a possible hysteresis mechanism may involve the presence of ss nicks in the DNA which allow a strand to melt and fray with time in the overstretched molecule (16). The existence of ss regions could account for the lower forces displayed at the same extension in the returning part of the stretching cycle. [Consistent with this model, a 1 M Na^+ buffer nearly eliminates the melting hysteresis without noticeably changing the force or cooperativity of

the transition (see below).] To further test this model, the strands of dsDNA were cross-linked with 4,5',8-trimethyl psoralen (one psoralen per ~ 20 bp). As seen in the top curve of Fig. 4, the intercalated psoralen eliminated the hysteresis in 150 mM Na^+ buffer, in support of the fraying model.

The effect of ionic strength on cross-linked molecules is also shown in Fig. 4. Very low ionic strength monovalent buffers had a marked effect on the transition force. The lower curves in Fig. 4 show the transition force dropping to ~ 45 pN in 0.6 mM Na^+ buffer. Smaller overstretching forces may be required at low ionic strengths because the electrostatic repulsion between phosphates favors the longer overstretched state. In 1 mM Mg^{2+} , however, the transition force remained high (65 pN), perhaps because condensed divalent counterions (17) more effectively reduced the DNA's charge. Hysteresis behavior reappeared in cross-linked molecules at very low salt. This behavior may simply involve melting of the unstacked bases without strand fraying. Base re-pairing might proceed slowly because repulsion between the phosphate backbones keeps the strands bowed outward. For most molecules, 1 mM Mg^{2+} buffer allows about as much melting hysteresis as 150 mM Na^+ buffer.

The narrow range of forces over which the overstretching transition occurs in native dsDNA (~ 2 pN in Fig. 2) indicates a highly cooperative process. Cooperativity implies that the overstretched regions are large and homogeneous and that they expand or contract only by converting base pairs at their boundaries with normal B-form regions; in other words, it must be energetically easier to spread an existing region than to nucleate a new one. The width of the overstretching

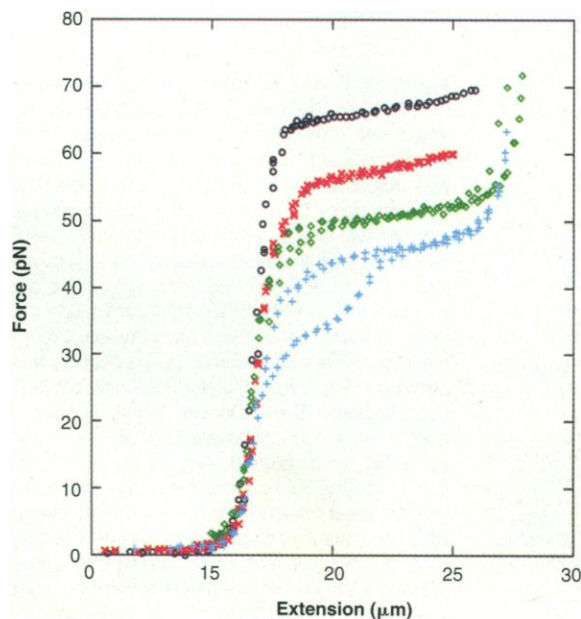


Fig. 4. Stretching of cross-linked dsDNA molecules in 150 mM NaCl, 10 mM tris, 1 mM EDTA, pH 8.0 buffer (black curve), Na_2EDTA buffer (pH 8) with Na^+ concentrations of 5 mM (red curve), 2.5 mM (green curve), and 0.625 mM (blue curve). For labeling dsDNA at both ends but on opposite strands, bio-11-dCTP (Sigma), dATP, dGTP, and dUTP were polymerized opposite λ 's 12-bp sticky ends using Klenow enzyme. For cross-linking studies, DNA was exposed to a saturated solution of 4,5',8-trimethyl psoralen and irradiated with ultraviolet light according to the method of Ussery *et al.* (29). This method should produce 5% intercalation of psoralen (30), and indeed the contour length was increased by $\sim 5\%$ over the molecule in Fig. 2.

transition is ~ 40 times narrower (in terms of force) than would be expected from a totally uncooperative process and ~ 3 times narrower (in terms of free energy ΔG) than thermal denaturation of dsDNA (18). The stretch transition must involve something more complex than simple base pair melting because opposite strands do not break apart. The molecules, which are attached by opposite strands to beads and often contain nicks, could not support stress when fully overstretched if large-scale melting occurred. Significantly, cross-linking reduced the cooperativity of the transition, as seen by the increased slope of the plateau of the top curve in Fig. 4 compared with the slope in Fig. 2. Psoralen sites may restrict the free movement of boundaries between B-form tracts and tracts of overstretched DNA, thus requiring extra nucleation sites to complete the transition.

The simplest model for the overstretching transition involves unwinding of the two strands to form an unstacked parallel ladder (Fig. 3B). However, the stacking interaction in mononucleotides and ssDNA is known to be noncooperative (19), so other molecular processes must be responsible for the high cooperativity of the transition. The cooperativity might arise by the propagation, throughout the molecule, of changes in its state of hydration, or its ionic atmosphere, or both. In this model, structurally relevant water on the surface of the molecule (20) may only form on long runs of B-form dsDNA. If the transition of a base pair into the overstretched form causes a long-range disruption of the water structure, then overstretching a neighboring base would be favored relative to creating a new disruption nucleus somewhere else in the molecule. Another model of the stretched form involves both unwinding of the chains

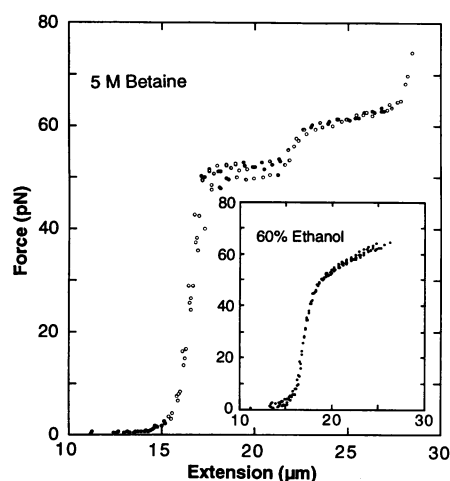


Fig. 5. Overstretching of λ -phage dsDNA in 5 M betaine (1-carboxy-*N,N,N*-trimethylmethaniminium hydroxide inner salt), 1 mM $MgCl_2$, 1 mM tris, pH 8. Inset: Overstretching of cross-linked λ -phage dsDNA in 60% ethanol, 2 mM NaCl, pH 8.

and slanting of the bases relative to the helix axis (Fig. 3B'). This "skewed ladder" proposed by Calladine and Drew (21) allows the bases to remain partially stacked. A considerable steric clash would then develop at the boundary with normal dsDNA; a molecule with mixed overstretched and unstretched regions would have higher energy than a molecule in which these regions have segregated to minimize the total number of junctions between regions.

An alternative source of cooperativity could involve changes in the ionic interactions of the molecule. Overstretching dsDNA will necessarily reduce its linear charge density resulting in the release of a number of ions from the condensation layer into the solution (17). Because ion condensation is a property of long charged polymers, the ionic release could couple adjacent and even distant parts of the molecule into a concerted transition. The molecular processes described above to explain the cooperativity of the overstretching transition are not exclusive of one another. All of them could, in fact, contribute to the sharpness of the transition.

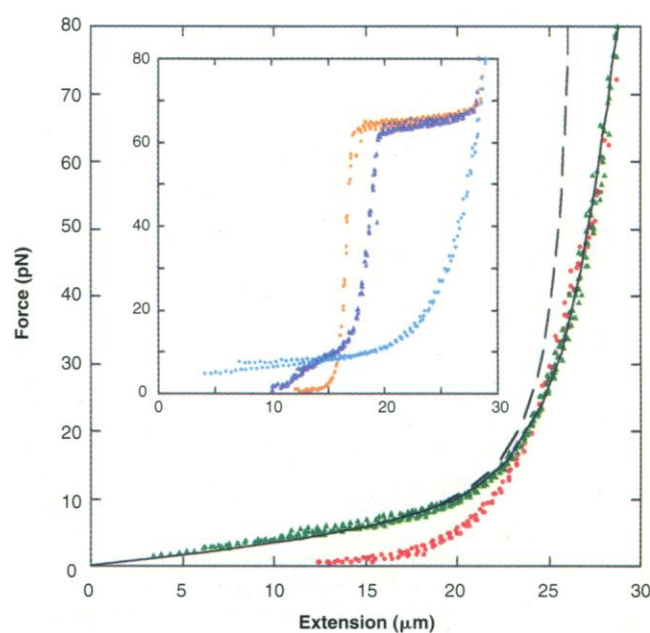
The suggestion that the cooperativity of the transition may involve changes in the hydration of the molecule is supported by the effect of ethanol and betaine. The reduced water activity in 60% ethanol almost eliminates the cooperativity (Fig. 5, inset). In 5 M betaine (Fig. 5), the molecule displays two transitions. The first involves

$\sim 40\%$ of the molecule and takes place at ~ 52 pN; the second occurs at ~ 60 pN. A λ DNA molecule is uniquely segregated into a left half with a $\sim 55\%$ GC content and a right half with a $\sim 45\%$ GC content (22); 5 M betaine could preferentially destabilize AT-rich regions over GC-rich regions (23). The first transition would then correspond to overstretching of the AT regions whereas the second would involve the overstretching of the GC-rich region.

In the stretch part of the stretch-relaxation cycle, certain molecules were permanently altered. Initially, a molecule would follow a dsDNA curve similar to that in Fig. 6 inset (orange) (where high salt eliminates hysteresis) but, after a few cycles in low salt buffer, the molecule would permanently switch to a different behavior (Fig. 6 inset, purple). Presumably these molecules had more than one nick in the same strand and under strain a whole section of one of the strands was lost. These molecules thus behave as ds and ss regions arranged in series.

These observations both confirm the molecular origin of the hysteresis behavior and suggested a way to study the elasticity of ssDNA molecules. In the experiments described above, the dsDNA molecules were biotin-labeled on opposite strands so that if the two strands separated completely by melting, the experiment ended. Changing the biotin label to opposite ends of the same strand, made it possible to melt off the unlabeled strand (with distilled water or

Fig. 6. A λ -phage ssDNA molecule was stretched in 150 mM NaCl, 10 mM tris, 1 mM EDTA, pH 8.0 (green curve). A different ssDNA molecule was stretched in 1 mM $Na_2.5$ EDTA, pH 8, 20% formaldehyde (red curve). The dashed line represents the elasticity of a freely jointed chain (FJC). The continuous line represents an FJC with stretch modulus. For labeling a ssDNA at both ends, two oligonucleotides were constructed, a 20-nucleotide (nt) strand complementary to the right overhang of λ , and a 5'-biotinylated 8 nt complementary to the remaining 8 bp of the 20 nt. These oligos were hybridized to each other and to the right end of λ and then ligated with T4 ligase. The left end of λ was then biotinylated with Klenow enzyme and bio-11-dCTP. Inset: Results from three different molecules tested in 1 M NaCl, 10 mM tris, 1 mM EDTA, pH 8.0. Orange curve: stretching of a λ -phage dsDNA molecule; purple curve: a molecule (previously stretched in low-salt buffer) that became partially ds and partially ss; and blue curve: stretching of a ssDNA molecule previously denatured in 20% formaldehyde, adjusted to pH 7 with 10 mM tris and NaOH. Note that at any given force, the extension of the ds-ss hybrid is the linear combination of the ds (orange) and ss (blue) forms (70% and 30%, respectively).



formaldehyde), leaving only a single phosphodiester polymer chain connecting the beads. The elasticity of such ssDNA (lower curves, Fig. 6, and blue curve, inset) is markedly different from that of dsDNA. Because it is very flexible, ssDNA is more contractile than dsDNA at low extensions (1). Notice, however, that the curves for ssDNA and dsDNA (overstretched form) are asymptotic to the same length at high forces. Therefore, the two strands in overstretched dsDNA probably cannot remain twisted around each other or else they would not be able to extend as far as ssDNA would do under the same force. Unwinding is possible because of the presence of nicks in the chains and the ability of the linker arm that tethers the biotin to act as a swivel.

It is often assumed that the elastic behavior of a single-chain polymer can be modeled as a freely jointed chain (FJC) of orientationally independent Kuhn segments. The green curve in Fig. 6 (150 mM Na⁺) can be fit only at low *Ex* by the FJC model by using a contour length L_{ss} of 27 μm and a Kuhn segment length b of 15 Å. This Kuhn length implies P being only 7.5 Å, which is shorter than commonly believed for ssDNA (24). However, the high-force behavior could not be matched with the simple Langevin function derived from this model (dashed curve in Fig. 6). A modified FJC model that incorporates Kuhn segments that can stretch as well as align under force was then tested (1):

$$Ex(F) = L_{ss} \left[\coth \left(\frac{Fb}{k_B T} \right) - \frac{k_B T}{Fb} \right] \left(1 + \frac{F}{S} \right)$$

where L_{ss} is a contour length, b is a Kuhn length, and S is the stretch modulus of ssDNA. For L_{ss} of 27 μm and a b of 15 Å, this expression fits the data with $S = 800$ pN (solid curve, Fig. 6). This observation suggests that the molecule undergoes a continuous conformational change throughout the extension cycle. One possible explanation is that the sugar pucker in ssDNA starts out as C3' *endo* which usually gives ~5.9 Å interphosphate distance (as in RNA) and accounts for the 27-μm contour length. The backbone transforms under tension into C2' *endo* pucker which usually has ~7 Å between phosphates (19). This change would account for the eventual stretch to 2.1 times B-form length as observed before (13, 14). The same high-force stretching is evident in the red curve of Fig. 6 (taken in 1 mM Na⁺ buffer). The model described above could not fit these low ionic strength data, which displayed a very low contractility at low forces. Electrostatic repulsion and excluded-volume probably account for this low-force behavior.

The sharp overstretching transition described here may have important implications

in the energetics of molecular processes that involve the deformation of the DNA molecule beyond its contour length. One such example is the energetics of the binding of RecA to dsDNA (25). To form the RecA–DNA filament, RecA must pay the energy cost required to overcome the entropic elasticity of the molecule and its overstretching to 1.5 times its contour length. Because binding of RecA does not require adenosine triphosphate hydrolysis, the energy to stretch the DNA molecule must be derived from the binding energy of the high-affinity form of the protein for DNA. Analysis of Fig. 2 indicates that the existence of the overstretching transition can greatly reduce the energy cost (the area under the *F-Ex* curve) to overstretch the DNA. Were the DNA molecule not to display the cooperative transition described here, but simply deform along a line extrapolated from the linear regime between 20 to 55 pN (Fig. 2), an additional 62×10^{-21} J (~15 $k_B T$) per RecA protein would be required to stretch DNA to 1.5 times its contour length. This energetic advantage is analogous to that suggested for the generation of kinks in DNA as an alternative to smooth bending deformations (26).

REFERENCES AND NOTES

1. S. B. Smith, L. Finzi, C. Bustamante, *Science* **258**, 1122 (1992).
2. C. Bustamante, J. Marko, E. Siggia, S. Smith, *ibid.* **265**, 1599 (1994).
3. A. Ashkin, J. M. Dziedzic, J. E. Bjorkholm, S. Chu, *Opt. Lett.* **11**, 288 (1986); K. Svoboda and S. Block, *Annu. Rev. Biophys. Biomol. Struct.* **23**, 247 (1994).
4. L. P. Ghislain, N. A. Switz, W. W. Webb, *Rev. Sci. Instrum.* **65**, 2762 (1994).
5. The force transducer is similar to that in (4) except that use of a dual-beam trap allows the use of beams that underfill the back aperture of the objective lenses, that is, the back aperture radius (R_{ba}) of the lens is 2.6 mm, while the $1/e^2$ radius of the gaussian laser beam is only 1.9 mm. This, in turn, permits collection of nearly all of the deflected light beam exiting the trap. The displacement X of the exiting beams, as seen by the position-sensitive detectors, is proportional to F on the bead by the relation:

$$F = (I/c) (NA) (X/R_{ba})$$
 where I is the intensity of the light beam and c is the speed of light (S. Smith *et al.*, in preparation). In accordance with this result, calibration of the force transducer has been shown by Stokes' law drag to be independent of the bead's size or of the buffer's refractive index.
6. At 50 pN, a typical molecule is 4.6% longer than an inextensible wormlike chain with a rise of 3.4 Å per base pair. As a linear approximation, the change in the length L in response to F could be given by $\Delta L/L = F/S$, where $S = 1087$ pN would be an intrinsic force modulus for single dsDNA molecules of any length. In terms of elastic deformation theory, a dsDNA molecule might be thought of as a rod with circular cross-sectional area $A = \pi R^2$ and made of a homogeneous material, for which the Young's modulus is $E = S/A = 3.46^{+/-} 0.3 \times 10^8$ Pa (for R of 10 Å). The bending rigidity of such a rod is $\kappa = EI$ were I , the cross-sectional area moment of inertia (7), is given by $I = \pi R^4/4$, $P = \kappa/k_B T$ (8). At 300 K, P would be 656 Å, or ~193 bp.
7. L. D. Landau and E. M. Lifshitz, *Theory of Elasticity* (Pergamon, Oxford, 1986), p. 67.
8. ———, *Statistical Physics Part. 1* (Pergamon, Oxford, ed. 3, 1980).
9. P. J. Hagerman, *Biopolymers* **20**, 1503 (1981); E. S. Sobel and J. A. Harpst, *ibid.* **31**, 1559 (1991).
10. There are three ways to reconcile this discrepancy. The simplest way is to propose that dsDNA adopts a slightly altered conformation for $F > 10$ pN, and the Young's modulus value cannot be extrapolated to B-form DNA. A second approach would be to model dsDNA as a round deformable rod that is not made of a homogeneous material but rather from stiff material on the inside (where the bases stack) and compliant material on the outside (along the phosphates). A reduced "radius of stiffness" could then be defined consistent with the 150-bp persistence length. Such reduced radius would be ~9 Å. A third explanation would retain the usually accepted radius for dsDNA (10 Å) and follow the suggestion of Trifonov and co-workers (11) that the stiffness of dsDNA, if it were inherently straight, would give it a persistence length of ~200 bp, but that the apparent persistence length is reduced to 150 bp by the presence of permanent bends along any random sequence of dsDNA. If such numerous bends really exist, then the value of dsDNA stiffness obtained here is close to agreement with that estimated from less direct methods.
11. E. N. Trifonov, R. K. Z. Tan, S. C. Harvey, in *DNA Bending and Curvature*, vol. 3 of *Structure and Expression*, W. K. Olson, R. H. Sarma, M. Sundaralingam, Eds. (Adenine, New York, 1987), pp. 243–253. See also J. A. Schellman and S. C. Harvey, *Biophys. Chem.* **55**, 95 (1995).
12. T. Thundat, D. P. Allison, R. J. Warmack, *Nucleic Acids. Res.* **22**, 4224 (1994).
13. I. Parra and B. Windle, *Nature Genet.* **5**, 17 (1993).
14. D. Bensimon, A. J. Simon, V. Croquette, A. Bensimon, *Phys. Rev. Lett.* **74**, 4754 (1995).
15. S. B. Smith, Y. Cui, A. C. Hausrath, C. Bustamante, *Biophys. J.* **68**, A250 (1995).
16. Because a stretch-relax cycle takes ~5 min, there is ample time for melting and reannealing to occur. Variability between molecules is due to the different placement and number of nicks.
17. G. R. Manning, *Q. Rev. Biophys.* **11**, 179 (1978).
18. The change in ΔG per base pair to convert to the overstretched form is $\Delta G = F\Delta X$, where F is 65 pN and the distance ΔX is the difference in rise per base pair during the transition. Thus $\Delta G = 9.3$ kJ/mol. If, with application of force, the base pairs were to unstack independently (without cooperativity), then the ratio of stacked to unstacked base pairs would equal $\exp(\Delta G - F\Delta X)/k_B T$. Because $k_B T$ is large (2.5 kJ/mol), the transition as a function of force would span 76 pN, with 10% conversion at 27 pN force, 50% at 65 pN, and 90% at 103 pN. The width of the melting transition for random sequence DNA is about 10 K. By using the relation $\Delta G = \Delta H - T\Delta S$ and assuming the enthalpy ΔH is independent of T , this transition width can be expressed as $\Delta\Delta G = \Delta T\Delta S = 850$ J mol⁻¹ bp⁻¹ for an entropy $\Delta S = 85$ J K⁻¹ mol⁻¹ [K. J. Breslauer, R. Frank, H. Blocker, L. A. Marky, *Proc. Natl. Acad. Sci. U.S.A.* **83**, 3746 (1986)]. The equivalent width of the overstretching transition is given by $\Delta\Delta G = \Delta F \Delta X = 2$ pN * 2.4 Å = 289 J mol⁻¹ bp⁻¹. Alternatively, overstretching might be treated as a first-order phase transition [H. B. Callen, *Thermodynamics and Introduction to Thermostatistics* (Wiley, New York, ed. 2, 1985); J. F. Marko and D. E. Siggia, *Macromolecules* **28**, 8759 (1995)]. At constant pressure, for a molecule of length L :

$$dG = -SdT - LdF$$
 At equilibrium, $-S_o dT - L_o dF = -S_B dT - L_B dF$, (where the subscripts indicate the o- and B forms). Then:

$$\frac{dF}{dT} = \frac{S_o - S_B}{L_o - L_B} = \frac{\Delta S}{\Delta L}$$
 This expression is the Clapeyron-Clausius equation for a system subjected to mechanical deformation. ΔS is then the discontinuous change in entropy accompanying the phase change and is proportional to the latent heat of the transition. Several processes may contribute to the entropy discontinuity, including the entropy change associated with the release of condensed ions and that associated with hydration changes in the molecule (see text).
19. W. Saenger, *Principles of Nucleic Acid Structure*

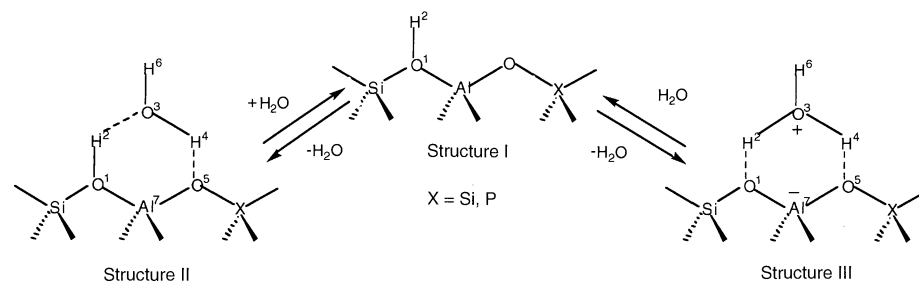
On the Nature of Water Bound to a Solid Acid Catalyst

L. Smith, A. K. Cheetham,* R. E. Morris, L. Marchese, J. M. Thomas,* P. A. Wright, J. Chen

The nature of the species formed when water interacts with Brønsted acid sites in a microporous solid acid catalyst, HSAPO-34, was studied by powder neutron diffraction and infrared spectroscopy. Previous infrared and computational studies had failed to unambiguously establish whether water is protonated to form hydronium (H_3O^+) ions or is merely hydrogen-bonded to acid sites inside the zeolite. Our experiments clearly showed that both species are present: An H_3O^+ ion is found in the eight-ring channel of the zeolite and a second water molecule is hydrogen-bonded to an acid site on the six-ring.

To understand more about the nature of the acid sites on solid catalysts is of both fundamental and profoundly practical importance. A probe molecule of more than academic interest in ascertaining the strength of the Brønsted acidity (proton-donating power) is water. Although the donating propensity of a bridging hydroxyl in aluminosilicate and silicoaluminophosphate (SAPO) catalysts (Scheme 1) is

known to be high, the most sophisticated quantum mechanical computations reveal (1) that no hydronium ions (structure III, Scheme 1) form, just hydrogen-bonded species (structure II, Scheme 1). Although some experimental studies may be interpreted in these terms (2), others (3) point strongly to the formation of H_3O^+ . Because solid (molecular sieve) catalysts are extensively used petrochemically (4) and are central in the design of superior materials for converting alkanes to branched-chain isomers of higher octane number, it is important to elucidate their Brønsted acidity.



Scheme 1

Here we show, by a combination of neutron diffraction and infrared (IR) spectroscopy, that H_3O^+ and hydrogen-bonded water coexist at the interior surface of a powerful new synthetic catalyst, HSAPO-34, which is structurally analogous to, but compositionally distinct from, the zeolitic mineral chabazite (5). Whereas in chabazite all the tetrahedral (T) sites are tenanted by either Si^{4+} or Al^{3+} ions, Al and P ions occupy the T sites alternately in HSAPO-34, and some Si ions reside in the sites

normally occupied by P. HSAPO-34 is acknowledged to be a powerful catalyst, with good performance in converting methanol to light alkenes (6).

In HSAPO-34, there are two distinct kinds of bridging hydroxyls, characterized by IR stretching frequencies at 3625 cm^{-1} (the so-called high-frequency mode) and at 3600 cm^{-1} (the low-frequency mode) (Fig. 1). This finding is in agreement with recent neutron diffraction studies of dehydrated HSAPO-34, which revealed protons at four-ring and six-ring oxygen sites (7). Our earlier diffuse reflectance IR Fourier transform spectroscopy (DRIFTS) measurements (3), allied to quantitative microgravimetry on progressively dehydrated HSAPO-34, indicated that, at room temperature, there is a stoichiometric proton transfer from one of the Brønsted sites to bound water, thereby forming H_3O^+ (structure III). Our interpretation concurred with that of Jentys *et al.* (8) but it contradicted that of Parker *et al.* (9),

- (Springer-Verlag, New York, 1984).
20. H. M. Berman, *Curr. Opin. Struct. Biol.* **4**, 345 (1994).
 21. C. R. Calladine and H. R. Drew, *Understanding DNA, the Molecule and How It Works* (Academic Press, London, 1992).
 22. N. Davidson and W. Szybalski, in *The Bacteriophage Lambda*, A. D. Hershey, Ed. (Cold Spring Harbor Laboratory, Cold Spring Harbor, NY, 1971), p. 56.
 23. Betaine has been shown to lower the melting temperatures of CG base pairs to the same value as that of AT base pairs [W. A. Rees, T. D. Yager, J. Korte, P. H. von Hippel, *Biochemistry* **32**, 137 (1993)]. Interestingly, the effect of betaine may have been just the opposite, that is, to enhance the difference between the forces required to induce the transition in AT- and CG-rich regions.
 24. The fitted Kuhn segment length of 15 Å implies a persistence length of 7.5 Å for ssDNA. This value is about half that estimated by E. K. Achter and G. Felsenfeld [*Biopolymers* **10**, 1625 (1971)] for apurinated ssDNA by using light scattering and sedimentation. It was assumed in that study that 1 M NaCl is a theta solvent for ssDNA. In the present study, the contractile force on a ssDNA molecule in 1 M NaCl, extrapolated to zero extension, was about 5 pN (see Fig. 6, inset blue). This force offset probably indicates secondary structure formation or condensation within the molecule. If such structure formed in the sedimentation studies, then an erroneously large value for the rigidity of ssDNA and for RNA could have been obtained.
 25. In the presence of adenosine triphosphate (ATP) or ATP[γ]S, RecA undergoes an allosteric change into a high-affinity form that binds dsDNA cooperatively in a stoichiometric ratio of 1 RecA/3 bp of dsDNA to form a right-handed helical filament [S. C. West, *Annu. Rev. Biochem.* **61**, 603 (1992)]. There are six RecA molecules and 18.6 bp/turn of the DNA molecule that is overstretched by a factor of 1.5 times its B-form contour length.
 26. A. Klug and F. H. C. Crick [*Nature* **255**, 530 (1975)] have suggested that formation of a few highly bent regions or "kinks" in DNA might be energetically favorable relative to smooth bending over a longer DNA length. The argument requires that after the ensuing of a localized kink in the DNA molecule, the energy required to bend the DNA further by an angle θ at that location, be smaller than the energy needed to bend the DNA by the same angle before the ensuing of the kink. This is indeed observed in macroscopic elastic media when the deformation goes beyond the elastic into the "plastic" regime (a plastic straw is a good example).
 27. Carboxylate-polystyrene beads (3.54 μm in diameter, CV = 2.7%, Spherotech) were covalently coated with streptavidin using 1-ethyl-3-(3-dimethylaminopropyl) carbodiimide (EDAC). Each molecule was pulled both right and left from the pipette to determine the point of attachment of the molecule on the pipette bead. Because the optically trapped bead can rotate freely, but the pipette-trapped bead cannot, *Ex* can be determined in absolute units (micrometers). In each *F-Ex* curve, data representing the following four processes is superimposed: extending the molecule to right of the pipette, then relaxing it from the right, extending it leftward, then relaxing it from the left. Each data point was taken after a ~0.5 μm change in extension and a 2-s waiting period. The force signal was then averaged for an additional 2 s and recorded. A complete right-left stretch cycle took about 10 min.
 28. A video showing actual bead-DNA-bead assembly (Fig. 1B) can be viewed on the World Wide Web at <<http://alice.uoregon.edu/~mark/>>.
 29. D. W. Ussery, R. W. Hoepfner, R. R. Sinden, *Methods Enzymol.* **212**, 242 (1992).
 30. J. E. Hearst, S. T. Isaacs, D. Kanne, H. Rapoport, K. Straub, *Q. Rev. Biophys.* **17**, 1 (1984).
 31. We thank D. Stigter, E. Siggia, J. Marko, and A. Hausrath for many useful discussions. This work was supported by NSF grants MBC 90118482 and BIR 9318945, and by NIH grant GM-32543. Partial support was provided by the Lucille P. Markey Foundation.

L. Smith, A. K. Cheetham, R. E. Morris, Materials Research Laboratory, University of California, Santa Barbara, CA 93106, USA.

L. Marchese, Dipartimento di Chimica I.F.M., Università degli Studi di Torino, 10125-Torino, Italy.

J. M. Thomas, P. A. Wright, J. Chen, Royal Institution of Great Britain, 21 Albemarle Street, London W1X 4BS, UK.

*To whom correspondence should be addressed.

15 December 1995; accepted 12 January 1996